Tellus (2004), 56B, 2–20
Printed in UK. All rights reserved

TELLUS

Aircraft Observation of CO_2, CO, O_3 and H_2 over the North Pacific during the PACE-7 Campaign

By Y. SAWA[1] *, H. MATSUEDA[1], Y. MAKINO[2], H. Y. INOUE[1], S. MURAYAMA[3], M. HIROTA[1], Y. TSUTSUMI[2], Y. ZAIZEN[1], M. IKEGAMI[1] and K. OKADA[1], [1]*Meteorological Research Institute, Tsukuba, Japan;* [2]*Japan Meteorological Agency, Tokyo, Japan;* [3]*National Institute of Advanced Industrial Science and Technology, Tsukuba, Japan*

(Manuscript received 2 July 2002; in final form 5 August 2003)

ABSTRACT

Aircraft observation under the Pacific Atmospheric Chemistry Experiment (PACE) program was performed from February 13 to 21, 2000 to examine in detail the distributions of CO_2 in the free troposphere between 5 and 11 km. Continuous measurements of CO_2 mixing ratios were made using an on-board measuring system over the northern North Pacific between Nagoya, Japan and Anchorage, Alaska, and the western North Pacific between Nagoya and Saipan. Other trace gases, such as CO and O_3, were also observed using continuous measuring systems at the same time. CO_2 over the northern Pacific (35°N and higher) showed highly variable mixing ratios, ranging from 374 ppm in the upper troposphere to 366 ppm in the lowermost stratosphere. This highly variable distribution of CO_2 was quite similar to that of CO, but the relationship between CO_2 and O_3 showed a strong negative correlation. These results indicated that the exchange process between the stratosphere and the troposphere significantly influences the large CO_2 variation. On the other hand, the CO_2 over the western North Pacific to the south of Japan showed no significant variation in the upper troposphere at 11 km but a relatively larger variability at 5 km. The CO_2 enhancement at lower altitudes coincided with the CO elevation due to the intrusion of a polluted air mass. Trajectory analysis indicated that the Asian continental outflow perturbed the CO_2 distributions over the western Pacific. Very low mixing ratios of O_3 of less than 20 ppb were distributed in the latitude band of 15–30°N at 11 km, reflecting the effects of transport from the equatorial region.

1. Introduction

Human activities, such as the burning of fossil fuels and changes in land use, have led to increased atmospheric concentrations of greenhouse gases, such as carbon dioxide (CO_2) and methane (CH_4). Mounting levels of greenhouse gases in the atmosphere are threatening to change the Earth's climate and weather, leading to gradual global warming. In addition, human activities contribute to an increase in the emissions of chemically active gases such as carbon monoxide (CO) and nitrogen oxides (NO_x) through the burning of fossil fuels and biomass. This increase enhances ozone (O_3) production in the troposphere, which accelerates future global warming because tropospheric O_3 is an important greenhouse gas. The increase in these long-lived and active gases, which are due to anthropogenic emissions, strongly affects the atmospheric environment through radiative forcing; it also affects the oxidative capacity of the atmosphere by a reaction with a reactive hydroxyl (OH) radical on a regional and global scale.

*Corresponding author.
e-mail: ysawa@mri-jma.go.jp

East Asia is a major source of anthropogenic trace gases and pollutants, which are increasing with the accelerated growth of the economy. Kato and Akimoto (1992) reported increases of NO_x and sulfur dioxide emissions from the East Asian region at a rate of 4% yr^{-1} from 1975 to 1987. Such high and rapidly growing emissions will have a significant impact on the chemistry of the atmosphere over the remote Pacific region. The long-range transport of materials in the troposphere from the continental regions of East Asia to the areas over the western Pacific has been demonstrated by chemical transport models (Berntsen et al., 1996; Wild and Akimoto, 2001).

Transport of Asian continental air containing enhanced CO, CH_4, aerosols and radon to the remote marine atmosphere has been reported on the basis of observational data at several sites in the North Pacific (e.g. Jaffe et al., 1997; Merrill et al., 1989; Balkanski et al., 1992; Harris et al., 1992; Bodhaine 1995). Recently, the PEM-West campaign was conducted over the western Pacific with the use of an aircraft to study the abundance and distribution of important trace gases and aerosols (Hoell et al., 1997). Ground level emissions were shown to be lofted to the upper troposphere by convective systems and transported to the remote Pacific and North America by rapid westerly advection

(e.g. Gregory et al., 1997; Talbot et al., 1997). These results suggest that human activities are having increasing influence on the atmosphere, even in regions that are remote from the emissions. In the North Pacific, flask sampling with aircraft has been used to examine the vertical and horizontal distributions of CO_2 over Japan (Tanaka et al., 1987; Nakazawa et al., 1993) and the western Pacific (Nakazawa et al., 1991; Matsueda et al., 2002). Surface distributions have been characterized at several long-term monitoring sites and from ships of opportunity (e.g. Conway et al., 1994; Francy et al., 1995; Keeling et al., 1995; Nakazawa et al., 1997; Novelli et al., 1997). However, knowledge of important chemical species over this region has been limited because of the very limited number of observations from the middle and upper troposphere.

The mixing ratios of CO_2 and other trace gases in the upper troposphere are determined in part by the exchanges of chemical compositions between the lowermost stratosphere and troposphere. Exchange of trace gases between the lowermost stratosphere and troposphere has been regarded as an important aspect of chemical transport in the atmosphere (e.g. Holton et al., 1995). Dynamic, chemical and radiative couplings between the stratosphere and the troposphere are important because the chemical effects from the stratosphere–troposphere exchange influence the radiative balance in the troposphere and lower stratosphere.

Some observational results of the effects on the mixing ratios over the North Pacific have been pointed out by Nakazawa et al. (1991) and Matsueda and Inoue (1996). A recent model study suggests that the stratosphere–troposphere exchange occurs relatively freely where isentropes cross the tropopause (Dethof et al., 2000). To study the exchange processes between the stratosphere and the troposphere, several studies conducted with the use of aircraft and on-board measuring systems have provided detailed information of the CO_2 distribution (Boering et al., 1994, 1996; Hintsa et al., 1998). However, few *in situ* observations of CO_2 and other trace gases in the near tropopause have been conducted over the western North Pacific, although intense ingress into the stratosphere in the latitudinal band 50°N–70°N and large zonal asymmetries have been pointed out in the regional patterns of the stratospheric–tropospheric exchange (Hoerling et al., 1993).

The Pacific Atmospheric Chemistry Experiment 7 (PACE-7) took place in February 2000 with an aircraft over the western North Pacific. The objectives of the PACE-7 campaign were: (1) to investigate the distribution of atmospheric trace gases and aerosols in the upper troposphere and lowermost stratosphere and the relationships among them over the northern part of the North Pacific and (2) to investigate the chemical composition of tropospheric air influenced by the Asian continental outflow over the subtropical Pacific regions to the south of Japan. The objective of this paper is to show the detailed distribution of atmospheric CO_2 that was measured continuously from onboard an aircraft from 13°N to 61°N at different altitudes (2–11 km). Other trace gases such as CO, O_3, H_2 and CH_4 were simultaneously measured to clarify the origin of the air masses. On the basis of these observational results, we discuss the exchange process between the troposphere and the stratosphere and the influence of the Asian outflow over the western North Pacific.

2. Experimental

2.1. Study area

A Gulfstream II aircraft was used to conduct the PACE-7 experiments over the North Pacific from February 13 to 21, 2000. The flight route of the campaign is shown in Fig. 1. The flight route was selected and divided into two phases with two focuses on the potential impact of the stratosphere–troposphere exchange and the impact of the Asian continental outflow. More detailed flight information was summarized in Table 1. The Gulfstream II departed from Nagoya airport (35°N, 137°E) in Japan for each phase of the PACE-7 project. For the first phase, four flights were conducted between Nagoya and Anchorage (61°N, 150°W) via Petropavlovsk (53°N, 158°E) at altitudes of 8 and 11 km for the northern region (>45°N). In addition, four flights were made over the southern region (<35°N) for the second phase between Nagoya and the three Pacific Islands of Naha (26°N, 127°E), Iwojima (25°N, 141°E) and Saipan (15°N, 146°E) at an altitude of 5 km to investigate the impact of the Asian continental outflow. A flight was also made at an altitude of 11 km between Nagoya and Saipan to survey the upper tropospheric air. To observe detailed vertical profiles for the southern region, three local flights were made near Naha, Iwojima and Saipan. These flights included short-level flights at altitudes of 2, 5, 8 and 11 km. Throughout the project, 12 flights totaling 42 h covered wide regions of the western North Pacific between 13°N and 61°N as well as the northern North Pacific between 125°E and 150°W.

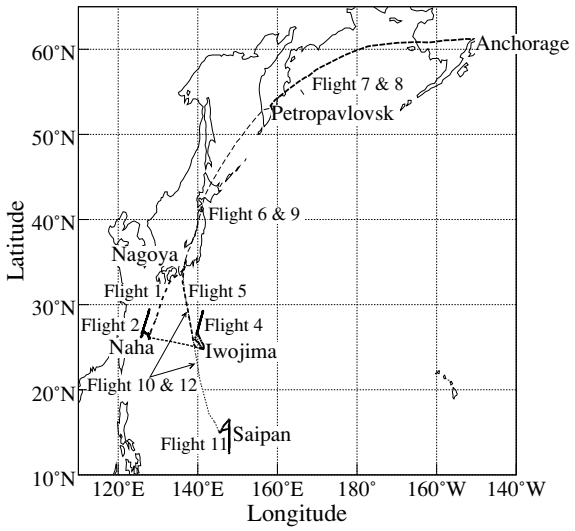

Fig 1. Aircraft flight route during the PACE-7 campaign from 13 to 21 February 2000.

Table 1. Summary of the PACE-7 flights

Flight no	Description start/end airport (latitude, longitude)	Main altitude	Start date time (UT)	End date time (UT)
1	Survey flight, Nagoya, Japan to Naha, Japan (35°N,137°E)–(26°N,128°E)	5 km	Feb. 13 02:50	Feb. 13 05:30
2	Local flight, Naha, Japan (26°N,128°E)	2, 5, 8 and 11 km	Feb. 13 06:30	Feb. 13 09:00
3	Survey flight, Naha, Japan to Iwojima, Japan (26°N,128°E)–(25°N,141°E)	5 km	Feb. 14 00:20	Feb. 14 02:35
4	Local flight, Iwojima, Japan (25°N,141°E)	2, 5, 8 and 11 km	Feb. 14 03:35	Feb. 14 07:00
5	Survey flight, Iwojima, Japan to Nagoya, Japan (25°N,141°E)–(35°N,137°E)	5 km	Feb. 14 07:50	Feb. 14 10:10
6	Survey flight, Nagoya, Japan to Petropavlovsk, Russia (35°N,137°E)–(53°N,158°E)	8 km	Feb. 17 00:35	Feb. 17 04:25
7	Survey flight, Petropavlovsk, Russia to Anchorage, USA (53°N,158°E)–(61°N,150°W)	8 km	Feb. 17 05:30	Feb. 17 09:45
8	Survey flight, Anchorage, USA to Petropavlovsk, Russia (61°N,150°W)–(53°N,158°E)	11 km	Feb. 18 18:15	Feb. 18 22:35
9	Survey flight, Petropavlovsk, Russia to Nagoya, Japan (53°N,158°E)–(35°N,137°E)	11 km → 5 km (<>45°N)	Feb. 18 23:30	Feb. 19 03:40
10	Survey flight, Nagoya, Japan to Saipan, Northern Marianas Island. (35°N,137°E)–(15°N,146°E)	5 km	Feb. 19 04:20	Feb. 19 08:30
11	Local flight, Saipan, Northern Marianas Island (15°N,146°E)	2, 5, 8, and 11 km	Feb. 19 23:55	Feb. 20 03:35
12	Survey flight, Saipan, Northern Marianas Island to Nagoya, Japan (15°N,146°E)–(35°N,137°E)	11 km	Feb. 20 23:55	Feb. 21 04:00

2.2. *Trace gas analysis*

2.2.1. Measuring system. Outside air was taken at a flow rate of 250×10^3 cm^3 min^{-1} from a stainless steel inlet mounted on the upper part of the aircraft body. A rotary vane pump (GAST, type 2567) was used. The air was divided through a manifold into several *in situ* measuring systems for CO_2, CO, H_2 and O_3 as well as into grab-sampling equipment for CH_4. Before the campaign, a leak test was conducted to confirm that the cabin air did not contaminate the sampled air outside of the aircraft. Aerosol concentration measurements and sample collections were conducted during the flights. In this paper, we mainly report on the measurements of trace gases. The aerosol data obtained during the campaign are discussed elsewhere.

The CO_2 concentration was measured onboard the aircraft using an NDIR (LI-COR, type LI-6252). The CO_2 measuring system was similar to that reported by Boering et al. (1994). The sampled air was introduced from the manifold to the measuring system by a diaphragm pump and then dried with an electric dehumidifier and chemical desiccant ($Mg(ClO_4)_2$). Although a mass-flow controller was used, the flow rate of sample air was variable around 400 ± 20 cm^3 min^{-1} due to the lower power for the diaphragm pump. Such variability of the flow rate did not affect the NDIR signal. The absolute pressure of the optical cell was kept constant by a pressure-control device to avoid a signal drift of the NDIR associated with the change in cabin pressure. During the flight campaign, the pressure of the optical cell was well controlled and changed by less than 2 hPa. Such a small variability in the air pressure was negligible because its effect on the precision of the NDIR was experimentally evaluated to be 0.02 ppm. From these results, the overall precision of the CO_2 measurement was estimated to be about ± 0.1 ppm. Several CO_2 measurements below 1.5 km were not used in this study because the air pressure in the NDIR cell was not well controlled for these low altitudes, due to an increase of the cabin pressure. Signals

of the NDIR instrument were collected by an analog-to-digital converter every second and 10-s averages were used for data analysis in this paper.

The CO concentration was measured with two different sets of onboard measuring instruments. In the first (the GC/HgO method), the CO and H_2 mixing ratios were measured every 3 min using a gas chromatograph equipped with a mercuric oxide reduction gas detector (Yanaco Co., Ltd., Japan, model TRA-1). This GC/HgO method has been reported in detail by Sawa et al. (1999). The analytical precision is about ± 2 ppb for CO and ± 5 ppb for H_2 in laboratory experiments, although analytical errors in measurements made onboard the aircraft were about twice as large due to the large vibration of the aircraft.

The second method used a reduction gas detector (Yanaco Co., Ltd, Japan, model TRD-1) to continuously measure CO in the air samples (the C/HgO method). This C/HgO measuring system was similar to that used in our previous campaign (Sawa et al., 1999). The dried air was passed through a pre-cut column (molecular sieve 13X) to remove HgO-sensitive gases such as hydrocarbons and aldehydes and then introduced to the hot HgO detector at 290 °C. The pressure-control device and mass-flow controller were used to maintain a constant pressure (1000 ± 5 hPa) and sample flow rate (100 ± 0.5 cm^3 min^{-1}). The response time of the C/HgO detector was estimated to be from 10 to 20 s when the CO mixing ratios changed to ± 50 ppb.

The ozone concentration was determined using an ultraviolet absorption instrument (Dylec Co., Ltd., Japan, 1007-AHJ). The concentration of ozone was calculated by a correction of the temperature and pressure of the sampled air. Ozone measurement was obtained every 12 s with a precision of about ± 2 ppb.

During this campaign, 22 air samples in 300 cm^3 stainless steel canisters were collected to measure the CH_4 mixing ratios. Most of the samples were obtained near Japan from 29°N to 43°N at altitudes of 5 and 8 km. A diaphragm pump was used to compress the sample air up to 1.8 kg cm^{-2}, and its CH_4 content was analyzed at the Meteorological Research Institute (MRI) after the campaign. The CH_4 mixing ratios were analyzed using a gas chromatograph equipped with a flame ionization detector (GC/FID) (Hirota et al., 1999). The precision in the GC/FID analysis was about 0.4%.

For the dew point temperature measurements, a three-stage frost-point hygrometer with a platinum resistance thermometer (Edge Tech, model 137) was used during the campaign. The accuracy of dew point temperature from this measurement was ± 1.0°C within a range of static air temperature from -70 to -30°C. Since there was a large error of the dew point temperature measurement for very dry air in high altitudes, only the data at altitudes below 8 km were used in this paper.

2.2.2. Calibration. The measuring systems were calibrated onboard the aircraft using three multi-component standard gases of CO_2 (348–381 ppm), CO (44–297 ppb) and H_2 (501–617 ppb) in air. They were prepared in 3 l aluminum high-pressure cylinders by a gas company (Taiyo Toyo Sanso Ltd, Japan). The CO_2 concentrations in the cylinders were determined against the standard gases in MRI that were assigned on the basis of the WMO CO_2 mole fraction scale propagated from the WMO central laboratory of NOAA/CMDL. These standard gases were introduced to the NDIR at an interval of 30 min to calibrate the measurements of air samples. No significant change of CO_2 content in any cylinders was found before and after the aircraft observations.

The CO and H_2 measurements in the GC/HgO method were calibrated every 18 min using the same standard gas cylinders. The CO and H_2 mixing ratios in these standard gases were assigned by gravimetric standards as described in Matsueda et al. (1998). For the C/HgO analysis, the standard gases were introduced to the instrument every 20 min. Since the differences between the C/HgO and GC/HgO were almost constant during each flight, the CO mixing ratios from the C/HgO were recalculated after subtracting the bias estimated during each flight. The C/HgO data after these corrections agreed well with the measured data from GC/HgO with a root mean square error of 9 ppb during this aircraft campaign. Not only the GC/HgO but also the C/HgO data provided useful information about detailed variability of CO during the campaign.

For the CH_4 calibration, the standard gas scale used here was higher than the NOAA/CMDL standard scale by 17.6 ± 3.0 ppb according to the comparison experiment in 1991. On the other hand, the O_3 instrument was calibrated at our laboratory before and after the campaign by an ozone calibration system using a Thermo Electron Model 49PS.

3. Results

3.1. *Meteorology overview*

The meteorology along the flight corridor strongly affects the distributions of all measured species. Thus, Fig. 2 shows mean pressure and wind fields at the surface and 500 hPa during the campaign from 13 to 21 February, 2000. This figure was created on the basis of the objective analysis data by the Japan Meteorological Agency. During this period of time, the major meteorological features were the Siberian High over Mongolia/Siberia and the Aleutian Low over the Pacific Ocean. This weather system was the typical pattern in the western North Pacific in the winter season. The pattern produced a strong northwesterly flow in the boundary layer along the Pacific Rim. This continental flow was found to be stronger from 15 to 17 and 21 in February. At 500 hPa, a strong westerly flow with a wind speed of more than 20 m s^{-1} was located in the mid-latitudinal zone between 20°N and 40°N. The subtropical jet stream was located around this region at 9–13 km with a maximum wind speed of $\sim$70 m s^{-1}. Several migratory cyclones were passing through the western Pacific Rim region from the west to the east. As an overall situation, these meteorological features indicated that the

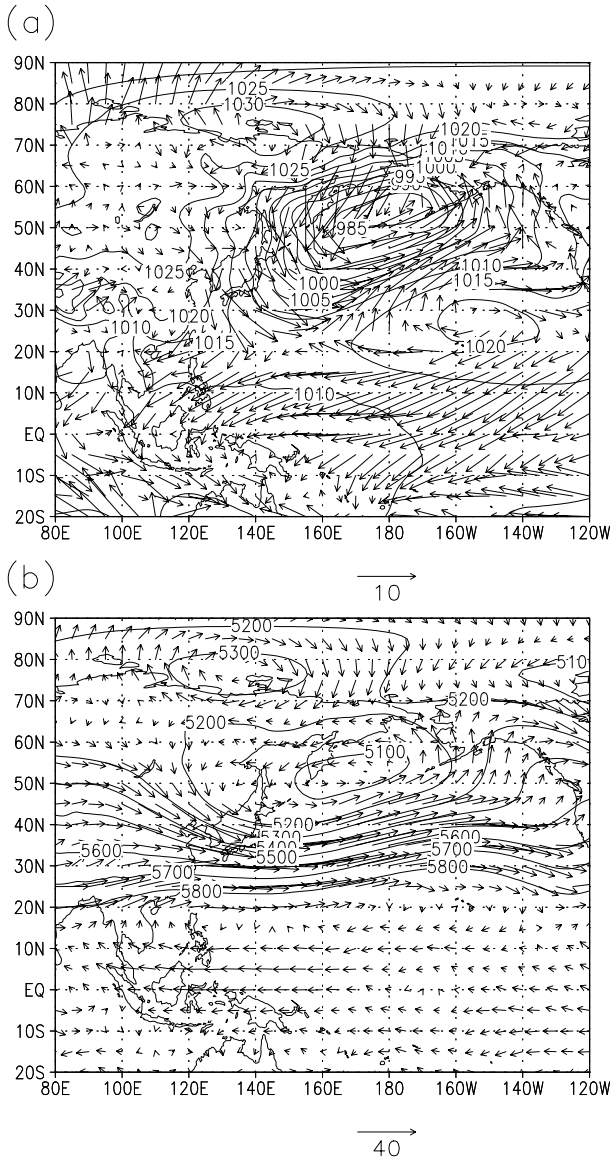

Fig 2. Mean pressure and wind fields during the campaign from 13 to 21 February, 2000 at (a) the surface and (b) 500 hPa. These distribution were calculated from the objected analysis data by the Japan Meteorological Agency (1.25×1.25 deg^2, 6 h).

western Pacific Ocean regions during this PACE-7 campaign were characterized by the strong air flow from the continent.

3.2. *Latitudinal distribution of CO_2*

The latitudinal distribution of the CO_2 mixing ratios between 13°N and 61°N is shown in Fig. 3a. These data were obtained during the level flights at 2, 5, 8 and 11 km. The approximate altitude of the tropopause was 8–9 km between 37°N and 61°N, while it was above 12 km in the southern region (<30°N) during the campaign. The CO_2 distribution observed during this campaign can be grouped into three characteristic regions of low (13°N–24°N), mid- (24°N–44°N) and high (44°N–61°N) latitudes. The CO_2 mixing ratios at low latitudes were nearly constant (368–370 ppm) for all altitudes from 2 to 11 km. The CO_2 level in this latitudinal band agreed well with that observed from JAL airliner observations (368–369 ppm) over the same area of the western North Pacific (Matsueda et al., 2001). In contrast, the CO_2 at mid- and high latitudes north of 24°N revealed vertical and temporal variation of their mixing ratios from 366 to 374 ppm. CO_2 at 11 km was similar to that at lower latitudes, but its mixing ratios increased with a decrease of altitude. In addition, a significant increase in the CO_2 level at 5 km was found among three different flights between 24°N and 35°N. At latitudes north of 44°N, a large variability from 366 to 374 ppm was observed at altitudes of 8 and 11 km. The lowest CO_2 mixing ratios during this campaign were found between 45°N and 53°N, and 61°N. The CO_2 mixing ratios measured during the campaign were in good agreement with the monthly values of February 2000 at NOAA/CMDL monitoring sites in low latitudes (370.08 ppm at Mauna Loa, and 370.24 ppm at Midway) (P. P. Tans and T. J. Conway from ftp.cmdl.noaa.gov/ccg/co2/flask; Conway et al., 1994). On the other hand, the mixing ratios observed in the upper troposphere at higher latitudes were significantly lower than those observed at Shemya (375.08 ppm) or Cold Bay (376.40 ppm), due to a large gradient of CO_2vertical profile.

3.3. *Latitudinal distribution of CO, O_3, CH_4 and H_2*

Figure 3b shows the latitudinal distribution of the CO mixing ratios during the level flights. The CO mixing ratios during this campaign showed quite a similar distribution to that of CO_2. The CO mixing ratios at low latitudes were nearly constant (70–100 ppb) for all altitudes from 2 to 11 km, while a large variability with higher mixing ratios up to 250 ppb was observed at mid-latitudes between 24°N and 44°N. At high latitudes, the CO showed a large variation from 40 to 200 ppb. The lowest CO mixing ratios of about 40 ppb corresponded to the lowest CO_2.

The latitudinal distribution of O_3 mixing ratios is shown in Fig. 3c. The O_3 mixing ratios at low latitudes between 13°N and 24°N showed nearly constant values of about 20–30 ppb. No significant difference in the O_3 profile from 2 to 11 km was observed at these low latitudes, although the O_3 at 8 km around 15°N showed a slight increase of around 70 ppb. Compared with the low latitudes, the O_3 mixing ratios at mid-latitudes between 24°N and 35°N showed slightly higher values of around 50 ppb at 2, 5 and 8 km. Largely enhanced O_3 mixing ratios of up to 110 ppb were only found around 27°N at 2 km. On the other hand, the mixing ratios at 11 km between 24°N and 30°N had relatively lower values of less than 30 ppb. It was of interest that extremely low O_3 mixing ratios of less than 10 ppb were detected between 26°N and 28°N at 11 km over the flights near Naha and Iwojima. At high latitudes, highly elevated O_3 from 100 to

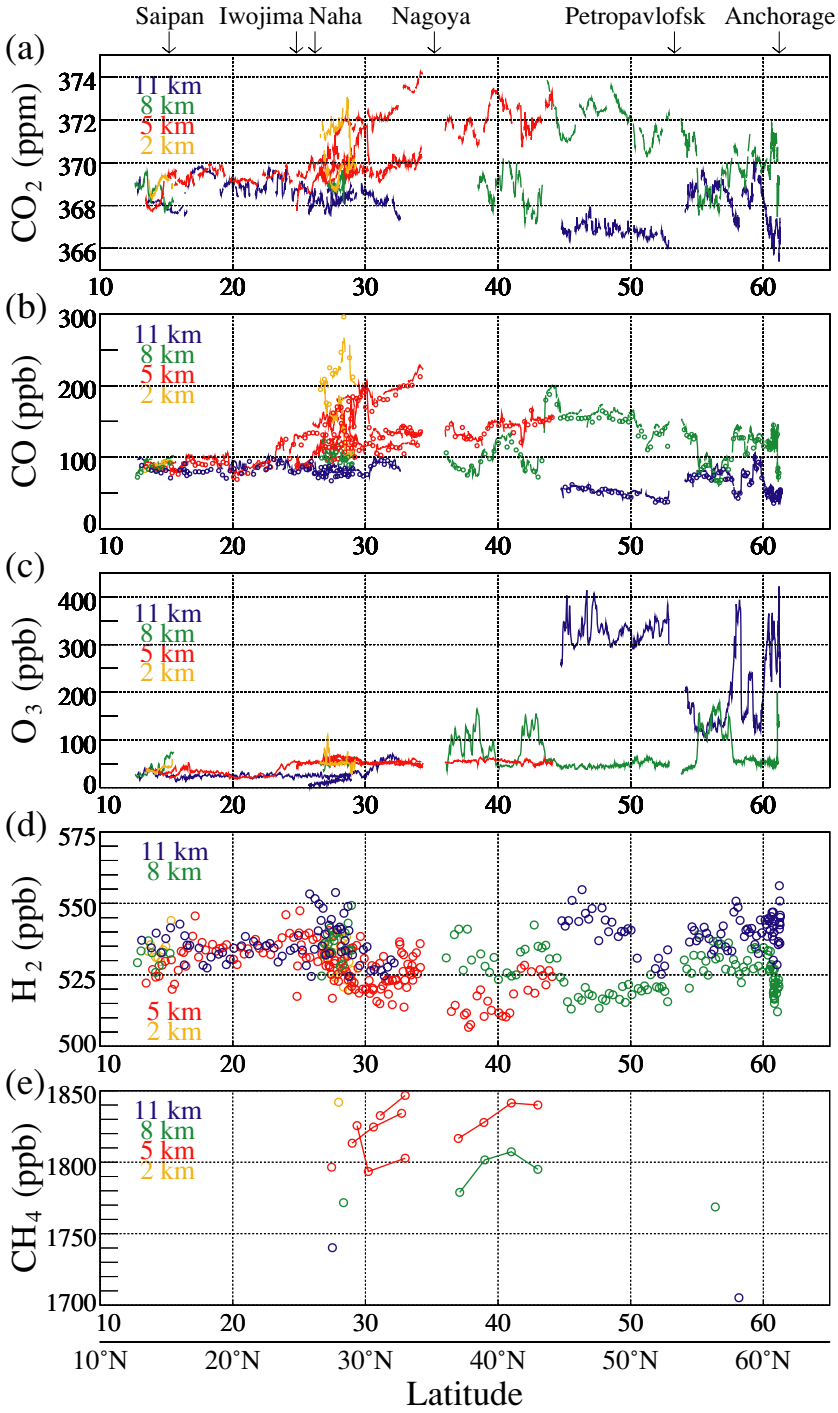

Fig 3. Latitudinal distributions of carbon dioxide (a) and carbon monoxide (b), ozone (c), hydrogen (d) and methane (e) mixing ratios over the North Pacific in February 2000. Data from level flights at 2, 5, 8 and 11 km are plotted.

400 ppb appeared at 11 km. Several O_3 increases of more than 70 ppb were also observed at 8 km, but the other O_3 measurements showed a low value of around 50 ppb.

The latitudinal distribution of H_2 mixing ratios is shown in Fig. 3d. At low latitudes between 13°N and 24°N, almost constant values of around 535 ppb were found at all altitudes from 2 to 11 km. On the other hand, the H_2 mixing ratios at mid-latitudes between 24°N and 35 °N varied from 510 to 555 ppb. Relatively lower H_2 mixing ratios in this region were observed at 5 km rather than at 8 or 11 km. At high latitudes between 45°N and 61°N, the H_2 mixing ratios were higher (535–560 ppb) at an altitude of 11 km than those (515–540 ppb) at an altitude of 8 km. This vertical increase of H_2 from 8 to 11 km was in contrast to the vertical decrease of CO_2 and CO with increasing altitude.

The results of CH_4 mixing ratios are plotted in Fig. 3e. The CH_4 showed a similar distribution pattern to those of CO_2 and CO, although the number of measurements was limited. The CH_4 mixing ratios observed during this campaign varied from 1700 to 1850 ppb.

4. Discussion

4.1. Variability of trace gas mixing ratios at altitudes of 8 and 11 km at high latitudes

4.1.1. Meteorology related to CO_2. At high latitudes between 36°N and 61°N, the overall mean of the CO_2 mixing ratios at 11 km was about 1–4 ppm lower than that at 8 km, although the difference between two altitudes was highly variable with time and space. The meteorology along the flight route strongly effected the distributions of CO_2 and other trace gases measured during these flights. This was illustrated by the cross-sections of the potential vorticity (PV), horizontal wind speed and the potential temperature (Figs. 4a and c). These figures were constructed from the objective analysis data by the Japan Meteorological Agency (JMA) (1.25 × 1.25 deg^2, 6 h). PV is a conservative tracer under adiabatic conditions and is typically much larger in the stratosphere than in the troposphere. Potential vorticity values in the range of 1.6 and 3.5 PVU ($\times 10^{-6}$ m^2 s^{-1} K kg^{-1}) have been associated previously with the dynamical tropopause (e.g. Hoskins et al., 1985; Hoerling et al., 1991). Some ambiguities remain about what value of PV is used in the determination of a tropopause height using PV. Thus, the thermal tropopause height was also calculated over this region by the objective analysis data. The thermal tropopause height over this northern North Pacific during these flights was calculated to be about 8–9 km, which corresponded to the PV values of 2.5–3.0 PVU. It is suggested that the observed air at 11 km was mainly located within the lowermost stratosphere at 2–3 km above the tropopause. On the other hand, the altitude at 8 km almost corresponded to the upper troposphere although this flight altitude was occasionally located above the tropopause. Thus, the difference in the mean CO_2 level between two altitudes mainly reflects the higher mixing ratios in the upper troposphere rather than in the lowermost stratosphere in February. A similar difference in the CO_2 level across tropopause was observed in the same season by airliner flights between Tokyo and Anchorage (Nakazawa et al., 1991).

The PV variations at both altitudes are negatively associated with the spatial distribution pattern of CO_2 (Figs. 4b and 4d).

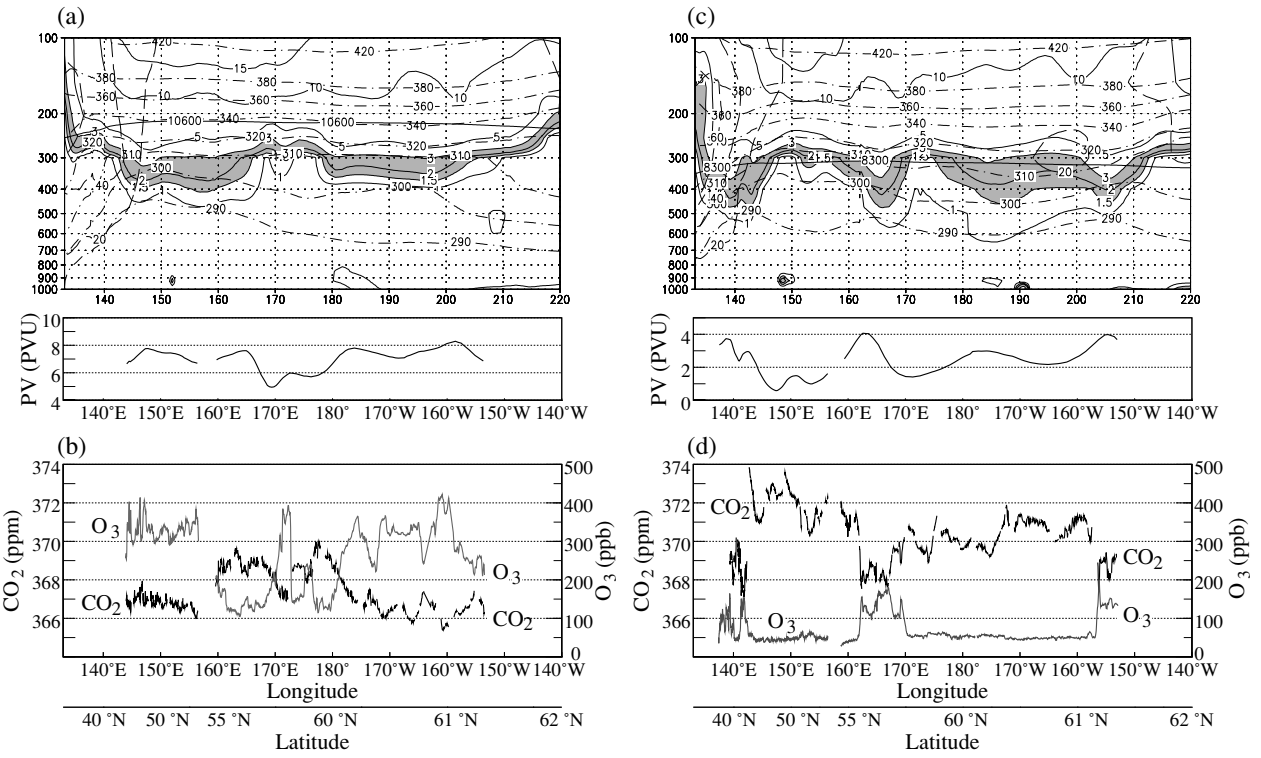

Fig 4. Cross section along the flights route of potential temperature (dash-dotted lines), potential vorticity PV (solid lines), highlighted area making PV values between 1.5 and 3 PVU and wind speed (dashed lines) on 19 February 2000 (a) and 17 February 2000 (c). Longitudinal distributions of PV along the flight level are also plotted. Longitudinal distributions of CO_2 and O_3 mixing ratios between Nagoya and Anchorage at altitude of 10.5–11 km on 19 February 2000 (Flight 8, 9) (b), and at altitude of 8 km on 17 February 2000 (Flight 6, 7) (d).

The relatively higher PV region with 7–9 PVU (180°–153°W) at 11 km almost corresponded to lower CO_2 mixing ratios of less than 367 ppm, while a relatively higher CO_2 level (367–370 ppm) appeared in the lower PV region with about 6 PVU (160°–180°E) over the Bering Sea. This negative relationship between the CO_2 and PV was also found at 8 km. The higher CO_2 above 372 ppm was observed at 8 km between 143°E and 162°E, while the other high CO_2 around 371 ppm was found between 172°W and 158°W (61°N) (Fig. 4d). These increased CO_2 were often found in air masses with high relative humidity. This result suggested that the CO_2 variability in the upper troposphere was largely related to a synoptic-scale weather perturbation, probably due to a change of Aleutian Low activities in the North Pacific. More detailed CO_2 distribution in the upper troposphere showed a characteristic variability on a spatial scale of about 250–400 km with amplitude of about 1–2 ppm. However, such variability could not be defined by the calculated PV, because of the lower resolution in the meteorological data. The other characteristic of the CO_2 distribution at 8 km was the fine variability on a spatial scale of about 40 km with amplitude of about 1 ppm. It was clearly revealed in sharply decreased CO_2 around 162°E, 169°E, 157°W and 154°W near the tropopause (Fig. 4d). Although a main cause for such fine variability could not be defined in this study, similar small-scale (50–100 km) variability of trace gases appearing around the tropopause height was also reported by Lelieveld et al. (1997).

4.1.2. CO_2–O_3 relation. Since O_3 increases from the troposphere to the stratosphere, a positive correlation between O_3 and PV was observed at altitudes of 8 and 11 km (Fig. 4). A similar relationship between PV and O_3 was also found in other studies (e.g. Folkins and Appenzeller 1996; Lelieveld et al., 1997; Brunner et al., 2001). Thus, ozone data observed in the same flights can be used as a good indicator to distinguish the upper tropospheric and lowermost stratospheric air (e.g. Parrish et al., 1998; Zahn et al., 2000, 2002). Folkins and Appenzeller (1996) pointed out a tight correlation between O_3 and CO_2 near the tropopause. In fact, a relationship between CO_2 and O_3 during our flights in the high latitude clearly showed that the detailed variations of the CO_2 at the both 8 and 11 km were correlated well with the O_3 mixing ratios (Fig. 5a). The low O_3 region with a constant level of about 50 ppb represented the upper troposphere, where the CO_2 showed higher mixing ratios ranging from 369 to 374 ppm.

In contrast, CO_2 mixing ratios of less than 369 ppm were found in the lowermost stratosphere that was roughly defined by higher O_3 mixing ratios of more than 70 ppb. In this lowermost stratosphere, the CO_2 mixing ratios decreased linearly with an increase of O_3. This relation showed a slope of -78 for $\Delta O_3/\Delta CO_2$. Such a linear negative correlation indicates a mixing line between two air masses in the lowermost stratosphere, one (the CO_2-poor air) having descended from the overworld of stratosphere, the other (the CO_2-rich air) from the upper troposphere. A similar compact negative CO_2–O_3 correlation in the lowermost stratosphere has also been reported by Hintsa et al. (1998) and Hoor et al. (2002), although no clear relation was observed just above the tropopause by Zahn et al. (1999). By interpreting the compact negative correlation to be the result of mixing across the tropopause, a CO_2 mixing ratio of the tropospheric end-member can be estimated by extrapolating the slope to an assigned tropopause value for O_3 (Hintsa et al., 1998; Hoor et al., 2002). Taking an O_3 threshold of 70 ppb for the upper

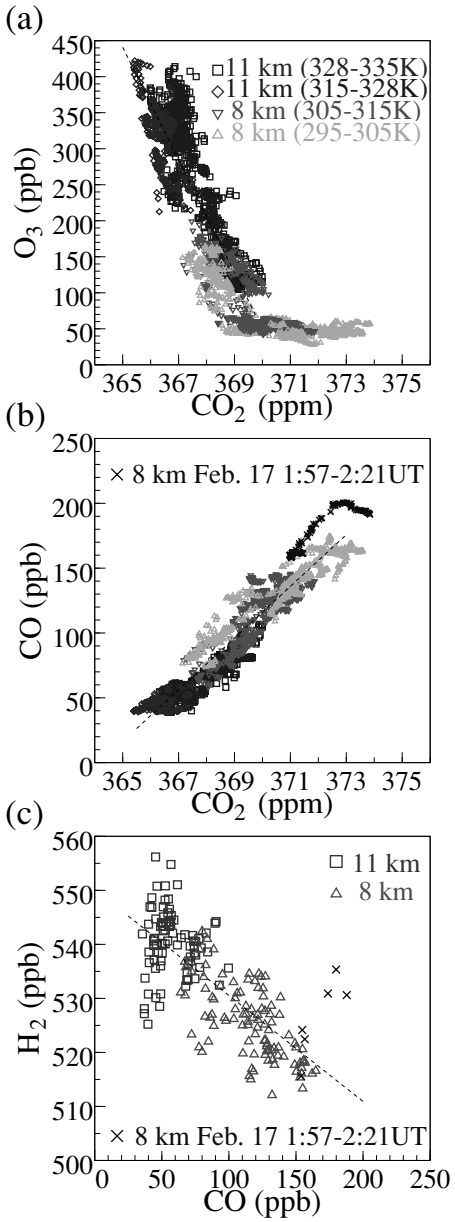

Fig 5. Correlation plots among the trace gases between Nagoya and Anchorage at 8 and 11 km in February 2000 (Flight 6–9). CO_2 and O_3(a), CO_2 and CO (b), CO and H_2 (c). Linear regression line is fitted to the data with O_3 mixing ratios above 70 ppb at 8 and 11 km (a). Linear regression lines are fitted to all data at 8 and 11 km (b) and (c).

troposphere, the corresponding CO_2 mixing ratios were between 368 and 370 ppm for the tropospheric end-member.

It is of interest that the CO_2–O_3 correlations in the lowermost stratosphere were clearly divided into several groups on the basis of the potential temperature (Fig. 5a). For example, the CO_2–O_3 correlation within the lower potential temperature (315–328 K) showed a different slope compared with that within the higher potential temperature (328–335 K). It was reported that isentropic stratosphere–troposphere exchange occurred vigorously on the lower isentropic surface (<330 K) using a transport model (Chen, 1995). These results suggested that an origin of air masses through isentropic stratosphere–troposphere exchange may be responsible for the slight different CO_2–O_3 correlation in the lowermost stratosphere. A similar difference in the relationship between CO_2 and O_3 depending on the potential temperature in the lowermost stratosphere has also been reported by Hoor et al. (2002).

4.1.3. CO_2–CO relation. The relationship between CO_2 and CO showed a strong positive correlation (Fig. 5b). This correlation showed no significant discontinuity across the tropopause corresponding to CO_2 mixing ratios between 368 and 370 ppm. Thus, the CO_2–CO correlation was almost approximated by a linear line with a slope of 0.02 for $\Delta CO/\Delta CO_2$. The slopes for the $\Delta CO/\Delta CO_2$ below and above the tropopause showed a similar value, although the data were slightly deviated in both layers. In the lowermost stratosphere, the CO_2–CO correlation largely depended on the potential temperature (Fig. 5b). The correlation was clearly divided into two groups of the higher (>315 K) and lower (<305 K) potential temperatures. The data in the intermediate potential temperature (305–315 K) distributed on the both correlations. These correlations in the lowermost stratosphere suggested two mixing lines with different air masses for the tropospheric end-member. Taking CO_2 thresholds of 368–370 ppm for the upper troposphere, the CO mixing ratios for the tropospheric end-members were estimated to be about 70–100 and 90–120 ppb for the higher (>315 K) and lower (<305 K) potential temperatures, respectively. These CO mixing ratios as tropospheric end-member were consistent with those estimated from O_3-CO negative correlations. These tropospheric mixing ratios with 70–120 ppb for CO and 368–370 ppm for CO_2 were similar to those in upper tropospheric air masses around subtropical regions south of 24°N, as shown in Fig 3. A similar result for the tropospheric end member was also obtained using the same multi-species relations among CO_2, CO and O_3 from the STREAM aircraft measurements (Hoor et al., 2002). From these results, it is probable that these subtropical air masses are mixed into the lowermost stratosphere near the subtropical jet through the isentropic cross-tropopause transport.

One more feature of the relationship between CO_2 and CO in the lowermost stratosphere is the insignificant decrease of CO at around 40–50 ppb in spite of the CO_2 decrease from about 367 to 365 ppm. This may be caused by a slow decrease of CO toward an equilibrium between CO destruction and the photochemical production of CO from CH_4 oxidation with the reaction of OH radicals in the upper part of the lowermost stratosphere. Lelieveld et al. (1997) estimated that the lower stratospheric CO mixing ratios from CH_4 oxidation is about 25 ppb. It is suggested that the CO observed at 11 km did not reach the equilibrium state between the CO destruction and production.

Exceptionally deviated data with elevated CO from 160 to 200 ppb were shown in the CO_2–CO correlation in the upper troposphere (Fig. 5b). These high mixing ratios were observed suddenly at 8 km around 43°N over the northern part of Japan from 1:57 to 2:21 UT on 17 February. The H_2 mixing ratios during the same period of time showed an increase from 515 to 535 ppb. The aerosol data in this region also showed an increase in the number of fine particles (diameter <0.1 μm) and the existence of soot in the aerosol samples. These results suggested that these air masses were emitted from the combustion source on the ground and intruded directly into the upper troposphere. Similar events with an abrupt increase of CO in the upper troposphere were also observed in several aircraft measurements over the western North Pacific (Koike et al., 1997; Talbot et al., 1997).

4.1.4. CO_2–H_2 and CO_2–CH_4 relations. The relationship between H_2 and CO at high latitudes clearly showed a negative correlation, although the data were scattered (Fig. 5c). This H_2–CO anti-correlation was almost approximated by a linear line with a slope of -0.19 for $\Delta H_2/\Delta CO$. A similar negative correlation was also found between H_2 and CO_2 in this region. Such relationships among H_2, CO_2 and CO are summarized in Table 2. The relationships between H_2 and other trace gases near the tropopause were not clearly found prior to the present study, because these were very limited measurements of vertical H_2 distributions (Ehhalt et al., 1977; Fabian et al., 1981).

The negative H_2–CO relationship indicated that H_2 mixing ratios were relatively lower in the upper troposphere than the lowermost stratosphere, but CO mixing ratios were relatively higher in the upper troposphere. In the troposphere, H_2 distributions showed significant seasonal and latitudinal variations due to a strong uptake by soil (Novelli et al., 1999; Simmonds et al., 2000; Yonemura et al., 2000). A recent study using a three-dimensional model indicated that a strong vertical gradient of H_2 result from the soil uptake (Hauglustaine and Ehhalt, 2002). On the other hand, H_2 in the stratosphere is produced photochemically through CH_4 oxidation (Dessler et al., 1994). These results suggested that strong sink in the lower troposphere as well as *in situ* H_2 production in the stratosphere is responsible for the difference in H_2 mixing ratios across the tropopause.

The relationships between CH_4 and other trace gases such as CO_2, CO and O_3 are also shown in Table 2. These were linearly correlated, although the number of measurements was limited. The ratios of increased CO to CH_4 mixing ratios were calculated to be about 1 and similar to the emission ratios observed in the air mass originated from urban/industrial pollution but different from those of biomass burning (Harriss et al., 1994;

Table 2. Measured correlation over the North Pacific between 36°N and 61°N at 8 and 11 km

Ratios	Slope	Coefficient of correlation	Number of data
$\Delta O_3/\Delta CO_2$ (ppb/ppm $O_3 > 70$ ppb)	−78	−0.88	1704
$\Delta O_3/\Delta CO$ (ppb/ppb $O_3 > 70$ ppb)	−4.6	−0.91	1760
$\Delta CO/\Delta CO_2$ (ppm/ppm)	0.019	0.95	2195
$\Delta H_2/\Delta CO_2$ (ppb/ppm)	−3.9	−0.75	187
$\Delta H_2/\Delta CO$ (ppb/ppb)	−0.19	−0.73	219
$\Delta CH_4/\Delta CO_2$(ppb/ppm)	40	0.92	5
$\Delta CH_4/\Delta CO$(ppb/ppb)	1.2	0.92	5
$\Delta CH_4/\Delta O_3$(ppb/ppb)	−0.31	−0.97	6

Matsueda and Inoue 1999). The backward trajectories for this region (37°N–43°N) show the westerly flows from the Asian continent, suggesting the influence of the Asian outflow. A negative relationship was found between CH_4 and O_3, reflecting the lower CH_4 and higher O_3 in the stratosphere.

4.2. *Effects of the Asian outflow*

4.2.1. Enhancement of CO_2 and CO at an altitude of 5 km at mid-latitudes. At mid-latitudes between 35°N and 24°N over the western North Pacific, a large change in the CO_2 mixing ratios at 5 km was observed among three level flights from Nagoya to Naha, Iwojima and Saipan (Fig. 6). A nearly flat distribution with relatively lower CO_2 of about 370 ppm was observed during Flight 1 on 13 February (Fig. 6a). These CO_2 values seemed to be background level at 5 km during this season. In contrast, the latitudinal distribution on 14 February (Flight 5) showed a different pattern (Fig. 6b), including two increased peaks with a maximum CO_2 of 372 ppm near 30°N and 27°N. A more significant enhancement of CO_2 from 372 to 374 ppm was found between 27°N and 34°N during the Flight 10 on 19 February (Fig. 6c), although the latitudes south of 24°N during this flight showed a lower CO_2 level of less than 370 ppm. These elevated CO_2 values at 5 km suggested the influence of Asian continental emissions.

To examine the transport of CO_2-rich air masses, we compared latitudinal variations of relative humidity calculated from dew point temperature and air temperature observed during the three flights at 5 km (Fig. 6). The high relative humidity during the Flights 5 and 10 was associated with the enhanced CO_2, while no elevation of relative humidity was observed during the Flight 1 without an increase of CO_2. These positive relationships suggested that air masses with high CO_2 and high humidity were transported upward from the surface of the CO_2 source region to 5 km. The backward trajectories for all three flights showed strong westerly flows from the Asian continent by the prevailing wind in this region. The weather chart combined with a satellite image during the campaign showed frequent passages of cold fronts accompanied by convective clouds that move eastward in western North Pacific Rim region around Japan. Thus, these results suggested that the upward air motion combined with the rapid horizontal transport brought CO_2-rich air masses from the continent over to the western Pacific Ocean.

The enhanced CO_2 observed during the two flights coincided with an increase of CO (Fig. 6). This increased CO showed relatively higher mixing ratios from 150 to 230 ppb, compared with a background level of 100–120 ppb in this region. Thus, the CO_2–CO plot clearly showed a strong positive correlation with a slope of about 0.03 for $\Delta CO/\Delta CO_2$ (Fig. 7). The enhanced CO_2 was also correlated positively to an increase of CH_4 mixing ratios observed during the same flights. The relationships between CO_2 and other trace gases such as CO and CH_4 in these flights are summarized in Table 3. The ratios of increased CO to CH_4 mixing ratios were calculated to be about 0.4, similar to the ratios of 0.3–0.8 observed in the air masses originated from urban/industrial sources (Harriss et al., 1994; Wofsy et al., 1994; Bakwin et al., 1995). These positive relations among CO_2, CO and CH_4 suggest that the air masses with increased CO_2 at an altitude of 5 km were significantly influenced by the Asian continental outflow of pollutants from the anthropogenic emissions through injection from the surface up to 5 km. In contrast, such increased CO_2 above 370 ppm was not found south of 24°N. It is suggested that the influence of the Asian outflow is most significant at mid-latitudes north of 24°N but not significant at low latitudes south of 24°N. Similar enhancements of CO or NO at mid-latitudes between 20°N and 30°N were also found in the latitudinal distribution below 8 km, reflecting the outflow from the western Pacific Rim (Crawford et al., 1997). It might be caused by large continental emissions located in this mid-latitude, where strong westerly winds from the continent to the Pacific were dominated (Fig. 2). It was pointed out that the frontal activity is a major driving force for export of Asian pollution to the Pacific Ocean from the observations during PEM-West B (Liu et al., 1997) and a simulation using a three-dimensional model (Bey et al., 2001).

4.2.2. Vertical distribution of CO_2 and CO enhancements at mid-latitudes. In order to deduce the vertical features of the Asian continental outflow, we examined vertical profiles from the local flights around Naha, Iwojima and Saipan (Fig. 8). Enhanced CO_2 and CO due to the Asian outflow were clearly observed in the vertical distributions of local flights near Naha and Iwojima.

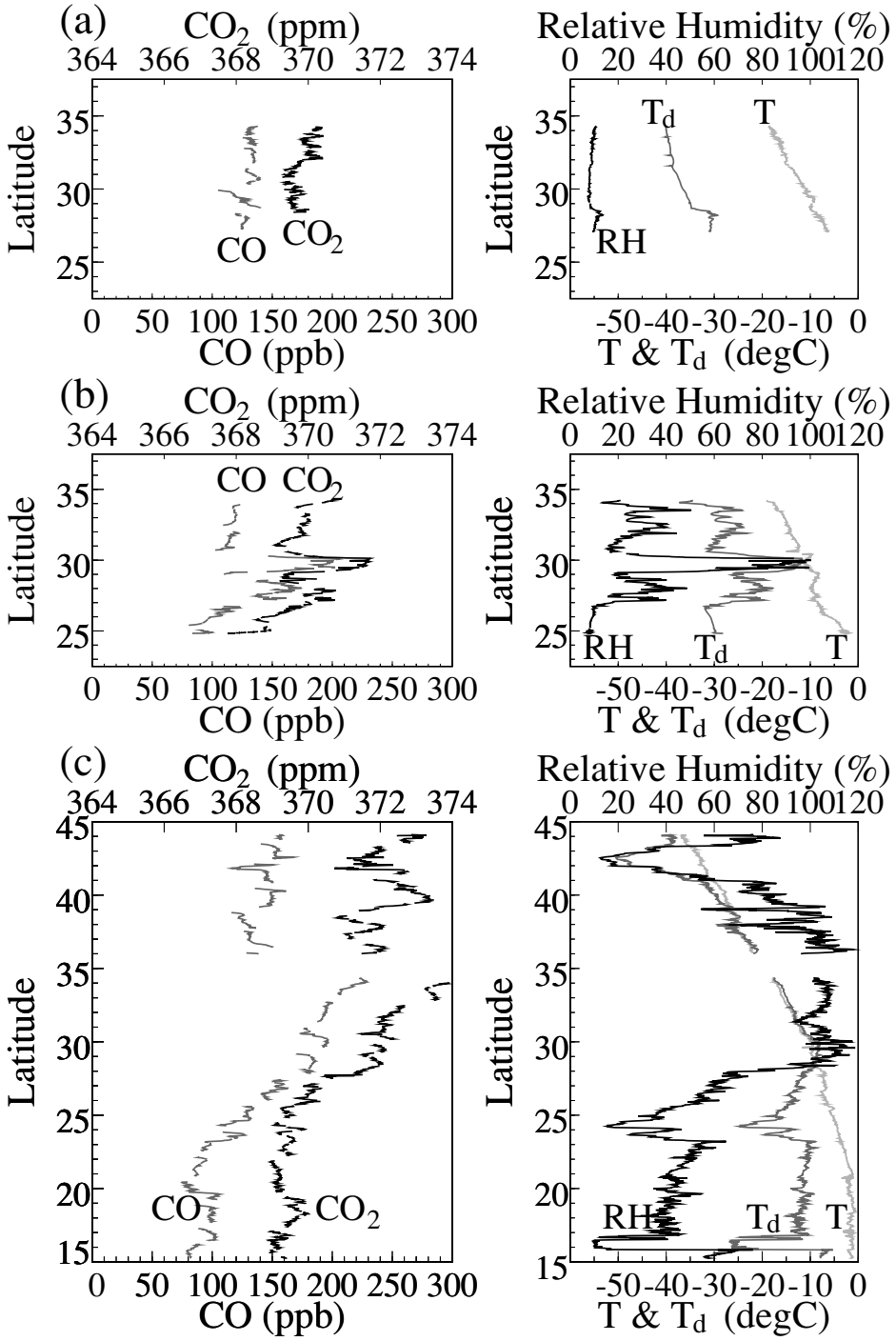

Fig 6. Latitudinal distribution of CO_2, and CO (left-hand panel), and temperature and dew point temperature and relative humidity (right-hand panel) on the flights at 5 km between Nagoya and Naha on 13 February, 2000 (Flight 1) (a), Iwojima and Nagoya on 14 February, 2000 (Flight 5) (b), and Nagoya and Saipan on 19 February, 2000 (Flight 10) (c).

The vertical distribution near Naha showed enhancements in the CO_2 and CO mixing ratios below an altitude of 4 km. The mixing ratios of both gases near Naha decreased with increasing altitude, suggesting a surface source. On the other hand, the vertical distribution near Iwojima showed a unique feature with the CO_2 and CO peaks at an altitude of around 4 km. The $\Delta CO/\Delta CO_2$ ratios were calculated to be about 0.03–0.04 for both flights, similar to the ratios found in the air masses originated from urban/industrial

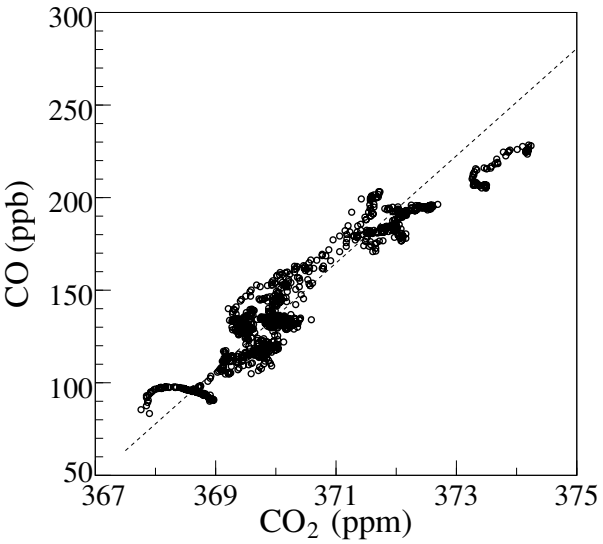

Fig 7. Correlation plot between CO_2 and CO between 24°N and 35°N at 5 km in February 2000 (Flight 1, 5, 10).

Table 3. Measured correlation over the western North Pacific between 24°N and 35°N at 5 km

Ratios	Slope	Coefficient of correlation	Number of data
$\Delta CO/\Delta CO_2$ (ppm/ppm)	0.029	0.89	631
$\Delta CH_4/\Delta CO_2$ (ppb/ppm)	9.8	0.95	5
$\Delta CH_4/\Delta CO$ (ppb/ppb)	0.40	0.78	8

sources. The relationship between CO and CH_4 observed near Naha also supported the anthropogenic sources because the ratio of $\Delta CH_4/\Delta CO$ (∼0.38) was similar to the emission ratios observed in the air masses influenced by urban/industrial pollution (Harriss et al., 1994; Wofsy et al., 1994; Bakwin et al., 1995; Matsueda and Inoue 1999).

Vertical profiles of air temperature and dew point temperature were examined to deduce vertical atmospheric structures for these local flights. The air-temperature profiles showed weak inversions at an altitude of about 4 km near Naha and of about 5 km near Iwojima. These layers were also confirmed as nearly saturated layers by the vertical profiles of dew point temperature observed near Naha and Iwojima. These results indicated that enhanced CO_2 and CO were confined to the area below the inversion layer, while the free tropospheric air above 5 km was not significantly influenced by continental pollution during our campaign in winter season. Kondo et al. (1997) also reported that significant enhancements of CO and NO_y were mainly observed in the boundary layer over the same area of the western Pacific in the same season.

The backward trajectories on the isentropic surface were calculated for 10 d, using the objective analysis data by the JMA (1.25×1.25 deg^2, 6 h). The trajectories in Fig. 9 were started at positions along the flight route at intervals of every 10 min at each altitude (2, 5, 8 and 11 km) for the three local flights. The trajectories for both flights near Naha and Iwojima showed the westerly flows from the Asian continent, but the distance from the continents to the observation area was different. While Flight 2 near Naha was conducted about 800 km off the eastern coast of the Asian continent, Flight 4 near Iwojima was conducted about 2000 km off the coast. Since the westerly winds in the surface layer were weak (<10 m s^{-1}) near Naha, high CO_2 and CO emitted from the Asian continent were transported slowly and accumulated in the surface air around the western Pacific Rim region. In contrast, compared to the vertical distribution near Naha, relatively larger enhancements of CO_2 and CO were found around 4 km near Iwojima but not in the surface air. Thus, it is suggested that the Asian continental pollution was rapidly transported to Iwojima through the higher altitude around 4 km because westerly winds at this higher altitude were much stronger (>30 m s^{-1}) than those near the surface air. The layer below 4 km near Iwojima was confirmed as nearly saturated layer by the vertical profiles of dew point temperature. It is most likely that convective pumping may play an important role in getting the pollutant from the surface air into the higher altitudes for the rapid long-range transport of Asian outflow to the remote Pacific region in winter.

The vertical distributions near Saipan showed relatively low and constant values of 368–370 ppm for CO_2 and 80–100 ppb for CO at all altitudes from 2 to 11 km. These profiles indicated that air was not influenced significantly by the continental outflow at this low latitude. The backward trajectories showed that these air masses at lower altitudes below 5 km originated from the central Pacific and were transported slowly by easterly flows (Fig. 9). These results suggested that the observed air at lower altitudes near Saipan was well-aged maritime air that had remained for at least 1 week over the central Pacific region. Although the trajectories at higher altitudes showed different flow patterns from those at lower altitudes, no significant increase was found in the vertical distribution of CO_2 and CO near Saipan. No large enhancements of CO and NO_y were observed in the middle troposphere at similar low latitudes either (Koike et al., 1997). These results suggested that there were no significant influences due to the Asian continental outflow in the southern part of the western North Pacific.

4.2.3. Enhancement of O_3 at mid- and low latitudes. In order to examine photochemical O_3 production in the continental air masses during the winter season, O_3 and CO at 2 and 5 km between 24°N and 35°N are plotted in Fig. 10. The tropospheric O_3 concentration showed almost constant values of around 50 ppb north of 24°N at 2 and 5 km. There was no significant correlation between O_3 and CO in this region, even if CO increased to 270 ppb. Poor correlation between CO and O_3 in the continental outflow with fresh polluted air was reported in winter by

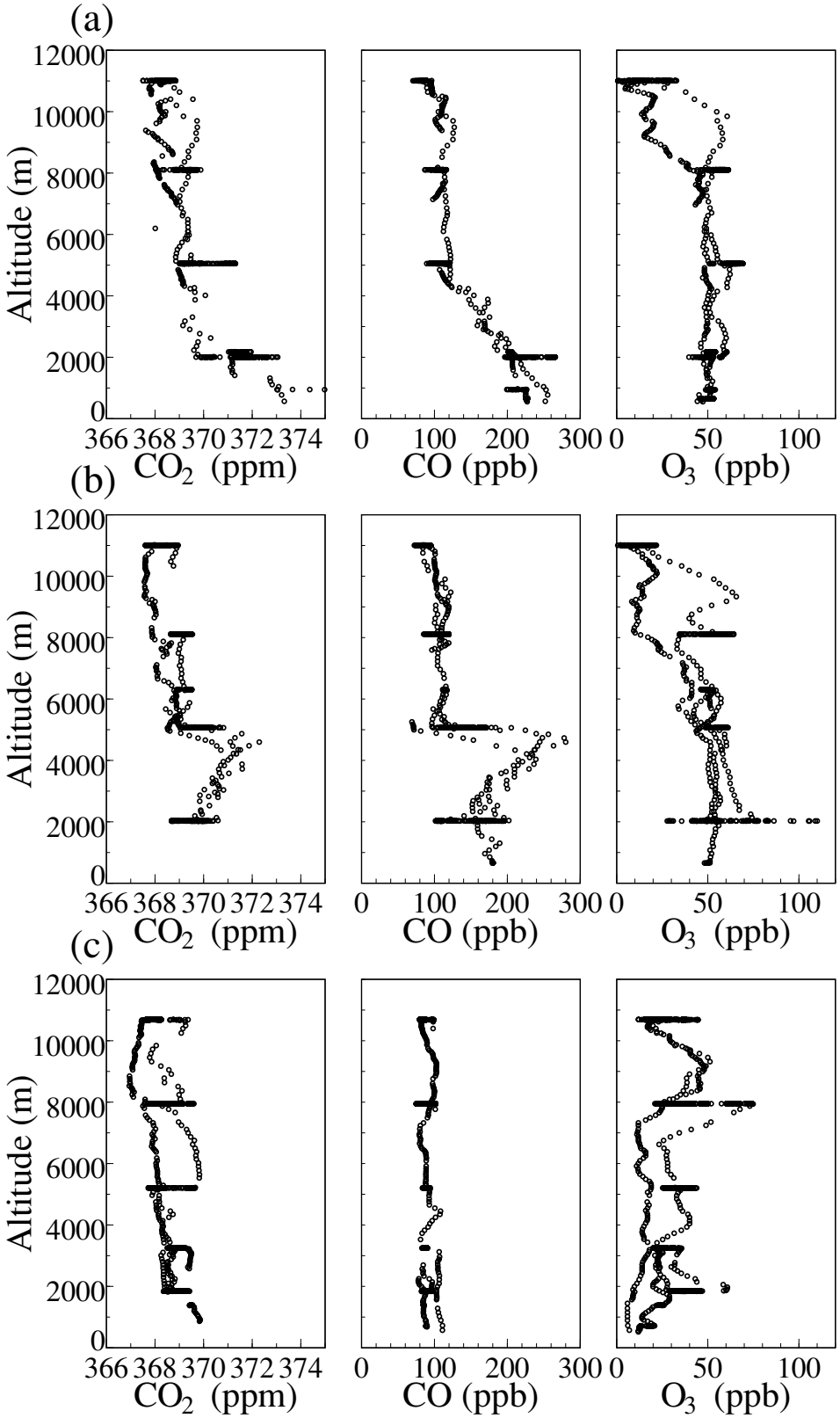

Fig 8. The profiles of CO_2, CO and O_3 mixing ratios of the local flight near Naha (Flight 2) (a), Iwojima (Flight 4) (b), and Saipan (Flight 11) (c).

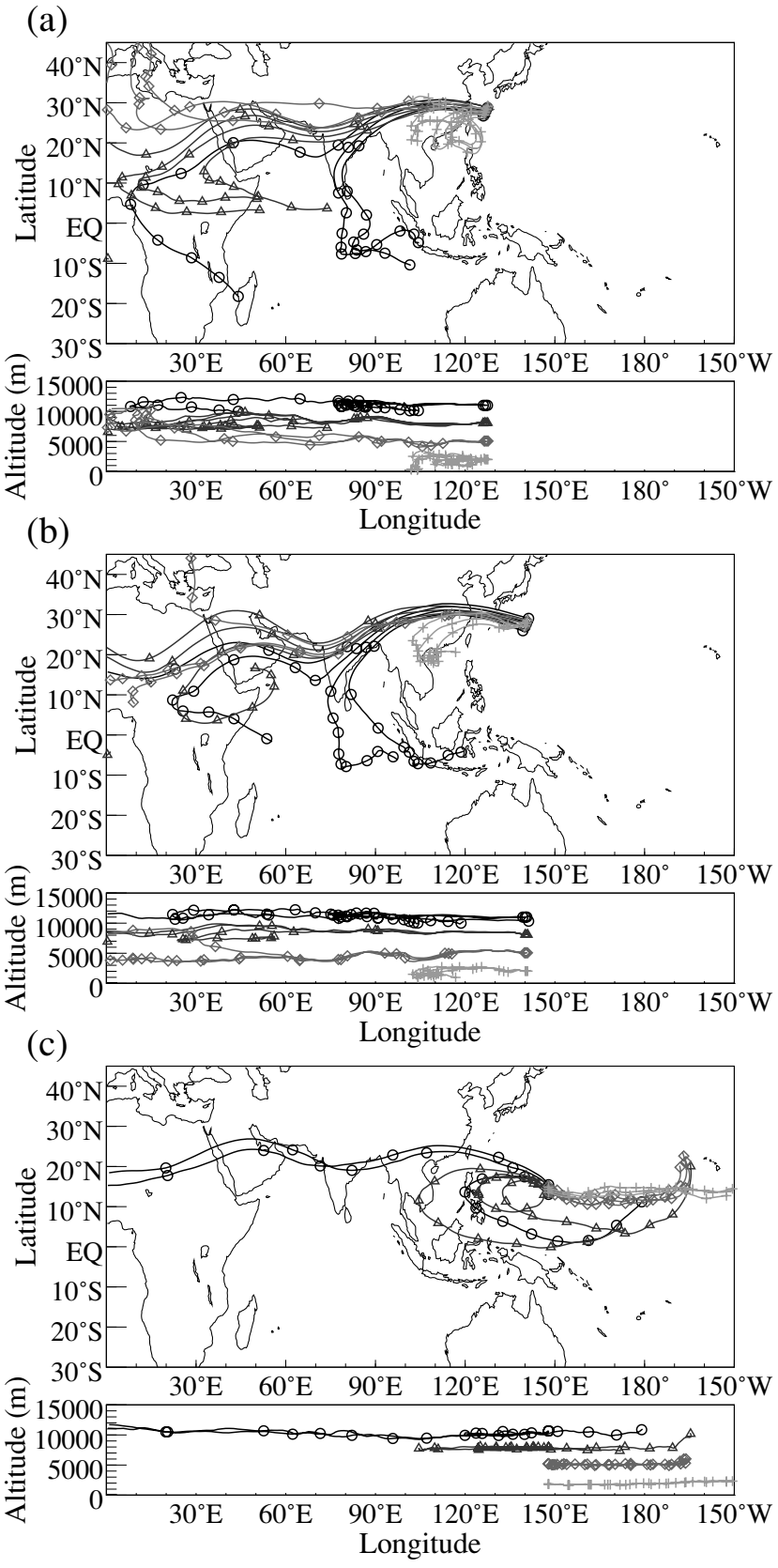

Fig 9. Isentropic backward trajectories of the local flights at four different altitudes (2, 5, 8 and 11 km) near Naha (Flight 2) (a), Iwojima (Flight 4) (b), and Saipan (Flight 11) (c). The circles, triangles, diamonds, and crosses along the trajectories indicate locations every 24 h intervals from sampling time at 11, 8, 5 and 2 km, respectively. The trajectories from the positions at intervals every 10 min for each flight level are plotted.

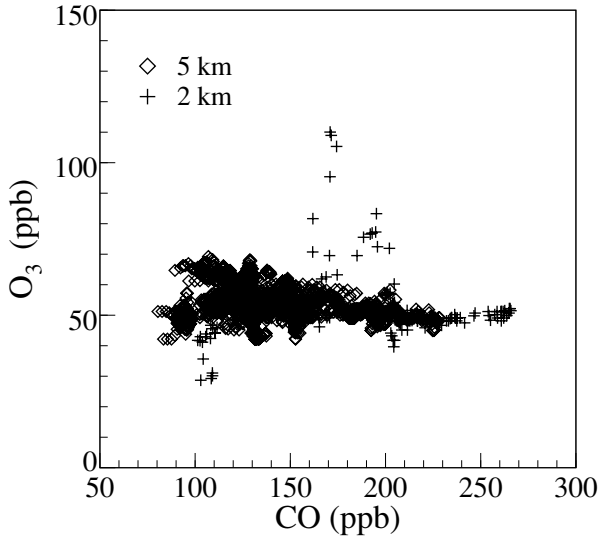

Fig 10. Correlation plot between CO and O_3 between 24°N and 35°N at 5 and 2 km in February 2000. Diamonds and crosses represent samples taken at 5 and 2 km, respectively.

Talbot et al. (1997). Koike et al. (1997) also reported a small difference in the O_3 mixing ratios for CO mixing ratios lower than 240 ppb and pointed out that the difference in O_3 mixing ratios depended on NO_y concentrations for the same CO mixing ratios in the lower troposphere during winter season. Overall, our observations in the free troposphere suggest a relatively smaller increase of O_3 compared with the CO increase in the boundary layer over the western Pacific during the winter season.

It is noted that there were several O_3 spikes with significantly enhanced mixing ratios of up to 110 ppb, but these high O_3 values were only found at an altitude of 2 km near Iwojima (Fig. 10). This enhancement suggests the photochemical production of O_3 in polluted air masses with higher CO mixing ratios of 170–220 ppb. On the other hand, relatively higher O_3 mixing ratios of around 80 ppb were found in the upper troposphere between altitudes of 7 and 10 km near Saipan at low latitudes (Fig. 8c), but these elevated O_3 values may not have originated from the photochemical production in the troposphere. When the O_3 mixing ratios at an altitude of 8 km increased from 30 to 80 ppb, the dew point temperature abruptly decreased from −30 to −45°C. These results suggested the effect of the intrusion of stratospheric air into this low latitude. In this region, the CO_2 mixing ratios showed a decrease from 369 to 368 ppm, although CO showed a small increase. Such O_3-rich and H_2O-poor air masses due to stratospheric intrusion were also found between 5 and 6 km at low altitudes (Wu et al., 1997), although the stratospheric influence on the composition of the troposphere over the western Pacific was mainly found at higher latitudes (Dibb et al., 1997).

4.3. Low O_3 mixing ratios in the subtropics

Extremely low O_3 of less than 10 ppb was found at 11 km between 26°N and 28°N during the level flights (Fig. 3c). The vertical profile near Naha revealed almost zero O_3 at 11 km and lower O_3 of less than 10 ppb above 9 km (Fig. 8a). A similar vertical distribution with very low O_3 of less than 10 ppb from 8 to 11 km was also observed near Iwojima (Fig. 8b). These low O_3 values in the upper troposphere appeared south of 28°N, although such low O_3 was not found north of 28°N. We carefully checked the analytical errors for these low O_3 data, but no signature indicating malfunction of ozone analyzer was found. Thus, these lowest O_3 mixing ratios were confirmed to be natural phenomenon. The lowest CO_2 and CO mixing ratios of about 368 and 80 ppb were observed at altitudes between 8 and 11 km near Naha and Iwojima (Fig. 8). Near-zero O_3 was found between 10 km and the tropopause over the equatorial Pacific (Kley et al., 1996) and at about 12 km at mid-latitudes (Davies et al., 1998) by balloon-borne soundings. However, there have been few observational results of extremely low O_3 into the upper troposphere in the subtropics.

In order to examine the origin of these extremely low O_3 values, the backward-trajectory analysis was conducted for the three local flights (Fig. 9). The trajectories at 11 km were different from those at lower altitudes. The backward trajectories at an altitude of 11 km near Naha and Iwojima clearly showed that air masses originated from the equatorial region west of Indonesia. These air masses drifted around the equatorial region for at least 1 week and were then rapidly transported to the western Pacific by a strong westerly wind within 3–4 d. The cloud images from Geostationary Meteorological Satellite 5 showed a large cluster of cumulonimbus over the equatorial region west of Indonesia at this time, suggesting strong upward motion of air from the surface to the upper troposphere by deep convection (Japan Meteorological Agency, 2000). These results suggested that the near-zero O_3 at 11 km in the subtropics over the western Pacific originated from the marine boundary air in the equatorial region.

Extremely low O_3 mixing ratios of less than 10 ppb have often been reported in the boundary layer in the tropical region (e.g. Routhier et al., 1980; Piotrowicz et al., 1986; Fishman et al., 1987; Singh et al., 1996). These low O_3 mixing ratios in the tropics are considered to be a result of net photochemical O_3 destruction in a low NO environment, sea surface deposition and little transport from the free troposphere (Singh et al., 1996). These results suggested that aged maritime air in the tropics is a main source of the extremely low O_3 in the upper troposphere in the subtropics.

During our campaign, not only near-zero O_3 but also lower O_3 of around 20 ppb was widespread at 11 km in the upper troposphere over the western Pacific from 15°N to 30°N. Over the equatorial Pacific in 0–14°N, similar low O_3 values of

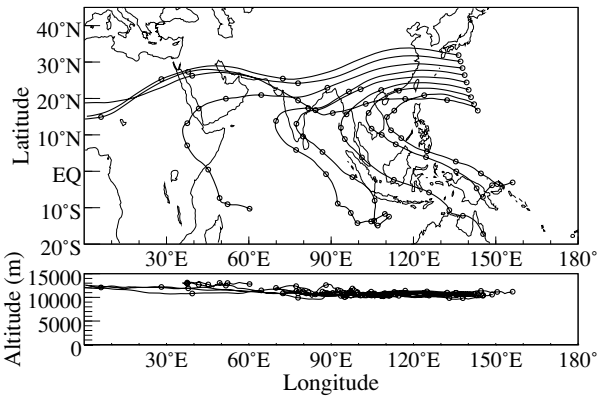

Fig 11. Isentropic backward trajectories for the flight from Saipan to Nagoya at 11 km (Flight 12). The circles along the trajectories indicate locations every 24 h intervals from sampling time at 11 km.

approximately 20 ppb were found at altitudes of 9–12 km during the PEM-West B campaign (Crawford et al., 1997; Kawakami et al., 1997; Talbot et al., 1997). All air masses with low O_3 at 11 km during our flights were also found to be transported by rapid flows from the equatorial regions according to the backward trajectories (Fig. 11). Thus, our observational results of low O_3 at 11 km indicated extensive vertical transport of the marine boundary layer to the upper troposphere by convective systems in the equatorial region and rapid horizontal transport in the upper troposphere from the equatorial to subtropical Pacific regions in winter. These results imply that rapid northward transport from the equatorial Pacific through the upper troposphere appears to be important for influencing the distributions of trace gases over the subtropical western North Pacific.

5. Conclusions

Continuous *in situ* measurements of CO_2, CO and O_3 mixing ratios were conducted over the North Pacific at various altitudes. The distributions and relationships among the gases over the western Pacific show large differences in their variability between the northern and southern regions studied. CO_2 over the northern Pacific ranged from 366 to 374 ppm, the variability can largely be explained by the exchange of stratospheric and tropospheric air.

The exchange process between stratospheric and tropospheric air dominates the mixing ratios of CO_2, CO and O_3 at higher (>8 km) altitudes in the northern Pacific north of 35°N. The mixing ratios of these species were changed on a scale of about 250–400 km even in the stratosphere and correlated well with each other. There was a difference of about 1–4 ppm in the CO_2 mixing ratios between the upper troposphere and the lowermost stratosphere. The CO_2 over the western North Pacific to the south of Japan showed a large variability at 5 km at mid-latitudes between 25°N and 35°N. CO_2 increases were apparent below a temperature inversion at an altitude of about 5 km. This enhancement at lower altitudes coincided with the CO elevation due to the intrusion of a polluted air mass from urban/industrial pollution. Most of the higher CO values above 150 ppb were observed in the southern region (<35°N) at lower altitudes (<5 km) in the PACE-7 campaign. On the other hand, the CO mixing ratios at high latitudes north of 35°N showed smaller variability between 110 and 160 ppb in the middle and upper troposphere. One exceptionally high CO value of up to 200 ppb was found between 43°N and 44°N at 8 km. At an altitude of 11 km, very low mixing ratios of O_3 distributed in the latitude band of 13–30°N, reflecting the effects of transport from the equatorial region.

Our PACE-7 campaign suggested that the trace gases over the western North Pacific in the winter season were largely influenced by: (1) the exchange between stratospheric and tropospheric air, (2) industrial/urban emission from the continent, (3) lower H_2 mixing ratios reflecting the land surface sink of H_2 and (4) low O_3 air relating to the uplift of clean, marine air and its transport into the northern hemisphere subtropical upper troposphere. These results could be obtained from the multi-species measurements in the same flight, although our aircraft campaign was limited somewhat by the sparseness of spatial and temporal coverage of the observations. Thus, further work is needed to better understand atmospheric trace gas cycles over the western North Pacific in the winter season.

6. Acknowledgments

The authors express their appreciation to the crewmembers and ground operation staff of the Diamond Air Service for providing flight facilities. We are also grateful to A. Kudo for his technical support with the measuring system. We are thankful to two anonymous reviewers for their many useful comments. This study was financially supported by the Science and Technology Agency of Japan.

References

Bakwin, P. S., Tans, P. P., Zhao, C., Ussler, W., III, and Quesnell, E. 1995. Measurements of carbon dioxide on a very tall tower. *Tellus* **47B**, 535–549.

Balkanski, Y. J., Jacob, D. J., Arimoto, R. and Kritz, M. A. 1992. Distribution of ^{222}Rn over the North Pacific: implications for continental influences. *J. Atmos. Chem.* **14**, 353–374.

Berntsen, T., Isaksen, I. S. A., Wang, W.-C. and Liang, X.-Z. 1996. Impact of increased anthropogenic emissions in Asia on tropospheric ozone and climate. *Tellus* **48B**, 13–32.

Bey, I., Jacob, D. J., Logan, J. A. and Yantosca, R. M. 2001. Asian chemical outflow to the Pacific in spring: origins, pathways, and budgets. *J. Geophys. Res.* **106**, 23 097–23 113.

Bodhaine, B. A. 1995. Aerosol absorption measurements at Barrow, Mauna Loa and the south pole. *J. Geophys. Res.* **100**, 8967–8975.

Boering, K. A., Daube, B. C., Jr, Wofsy, S. C., Loewenstein, M., Podolske, J. R. and Keim, E. R. 1994. Tracer–tracer relationships and lower stratospheric dynamics: CO_2 and N_2O correlations during SPADE. *Geophys. Res. Lett.* **23**, 2567–2570.

Boering, K. A., Wofsy, S. C., Daube, B. C., Schneider, H. R., Loewenstein, M., Podolske, J. R. and Conway, T. J. 1996. Stratospheric mean ages and transport rates from observations of carbon dioxide and nitrous oxide. *Science* **274**, 1340–1343.

Brunner, D., Staehelin, J., Jeker, D., Wernli, H. and Schumann, U. 2001. Nitrogen oxides and ozone in the tropopause region of the Northern Hemisphere: measurements from commercial aircraft in 1995/1996 and 1997. *J. Geophys. Res.* **106**, 27 673–27 699.

Chen, P. 1995. Isentropic cross-tropopause mass exchange in the extratropics. *J. Geophys. Res.* **100**, 16 661–16 673.

Conway, T. J., Tans, P. P., Waterman, L. S., Thoning, K. W., Kitzis, D. R., Masarie, K. A. and Zhang, N. 1994. Evidence for international variability of the carbon cycle from the National Oceanic and Atmospheric Administration/Climate Monitoring and Diagnostics Laboratory global air sampling network. *J. Geophys. Res.* **99**, 22 831–22 855.

Crawford, J., Davis, D., Chen, G, Bradshaw, J., Sandholm, S., Kondo, Y., Liu, S., Browell, E., Gregory, G., Anderson, B., Sachse, G., Collins, J., Barrick, J., Blake, D., Talbot, R. and Singh, H. 1997. An assessment of ozone photochemistry in the extratropical western North Pacific: impact of continental outflow during the late winter/early spring. *J. Geophys. Res.* **102**, 28 469–28 487.

Davies, W. E., Vaughan, G. and O'Connor, F. M. 1998. Observation of near-zero ozone concentrations in the upper troposphere at mid-latitudes. *Geophys. Res. Lett.* **25**, 1173–1176.

Dessler, A. E., Weinstock, E. M., Hintsa, E. J., Anderson, J. G., Webster, C. R., May, R. D., Elkins, J. W. and Dutton, G. S. 1994. An examination of the total hydrogen budget of the lower stratosphere. *Geophys. Res. Lett.* **21**, 2563–2566.

Dethof, A., O'Neill, A. and Slingo, J. 2000. Quantification of the isentropic mass transport across the dynamical tropopause. *J. Geophys. Res.* **105**, 12 279–12 293.

Dibb, J. E., Talbot, R. W., Lefer, B. L., Gregory, G. L., Browell, E. V., Bradshaw, J. D., Sandholm, S. T. and Singh, H. B. 1997. Distributions of beryllium 7 and lead 210, and soluble aerosol-associated ionic species over the western Pacific: PEM West B, February–March 1994. *J. Geophys. Res.* **102**, 28 287–28 302.

Ehhalt, D. H., Schmidt, U. and Heidt, L. E. 1977. Vertical profile of molecular hydrogen in the troposphere and stratosphere. *J. Geophys. Res.* **82**, 5907–5911.

Fabian, P., Borchers, R., Flentje, G., Matthews, W. A., Seiler, W., Giehl, H., Bunse, K., Müller, F., Schmidt, U., Volz, A., Khedim, A. and Johnen, F. J. 1981. The vertical distribution of stable trace gases at mid-latitudes. *J. Geophys. Res.* **86**, 5179–5184.

Fishman, J., Gregory, G. L., Sachse, G. W., Beck, S. M. and Hill, G. F. 1987. Vertical profiles of ozone, carbon monoxide, and dew point temperature observed during GTE/CITE 1. October–November 1983. *J. Geophys. Res.* **92**, 2083–2094.

Folkins, I. and Appenzeller, C. 1996. Ozone and potential vorticity at the subtropical tropopause break. *J. Geophys. Res.* **101**, 18 787–18 792.

Francy, R. J., Tans, P. P., Allison, C. E., Enting, I. G., White, J. W. and Troller, M. 1995. Changes in oceanic and terrestrial carbon uptake since 1982. *Nature* **373**, 326–330.

Gregory, G. L., Merrill, J. T., Shipham, M. C., Blake, D. R., Sachse, G. W. and Singh, H. B. 1997. Chemical characteristics of tropospheric air over the Pacific Ocean as measured during PEM-West B: relationship to Asian outflow and trajectory history. *J. Geophys. Res.* **102**, 28 275–28 285.

Hauglustaine, D. A. and Ehhalt, D. H. 2002. A three-dimensional model of molecular hydrogen in the troposphere. *J. Geophys. Res.* **107**, doi 10.1029/2001JD001156.

Harris, J. M., Tans, P. P., Dlugokencky, E. J., Masarie, K. A., Lang, P. M., Whittlestone, S. and Steele, P. 1992. Variations in atmospheric methane at Mauna Loa observatory related to long-range transport. *J. Geophys. Res.* **97**, 6003–6010.

Harriss, R. C., Sachse, G. W., Collins J. E. Jr, Wade, L., Bartlett, K. B., Talbot, R. W., Browell, E. V., Barrie, L. A., Hill, G. F. and Burney, L. G. 1994. Carbon monoxide and methane over Canada: July–August 1990. *J. Geophys. Res.* **99**, 1659–1669.

Hintsa, E. J., Boering, K. A., Weinstock, E. M., Anderson, J. G., Gary, B. L., Pfister, L., Daube, B. C., Wofsy, S. C., Loewenstein, M., Podolske, J. R., Margitan, J. J. and Bui, T. P. 1998. Troposphere-to-stratosphere transport in the lowermost stratosphere from measurements of H_2O, CO_2, N_2O and O_3. *Geophys. Res. Lett.* **25**, 2655–2658

Hirota, M., Tsutsumi, Y., Makino, Y., Sasaki, T., Zaizen, Y. and Ikegami, M. 1999. Variation and long-term trends in tropospheric methane (CH_4) concentration over Japan since 1986. *Pap. Met. Geophys.* **49**, 43–58.

Hoell, J. M. Davis, D. D., Liu, S. C., Newell, R. E., Akimoto, H., McNeal, R. J. and Bendura, R. J. 1997. The Pacific Exploratory Mission-West Phase B: February–March, 1994. *J. Geophys. Res.* **102**, 28 223–28 239.

Hoerling, M. P., Schaack, T. K. and Lenzen, A. J. 1991. Global objective tropopause analysis. *Mon. Wea. Rev.* **119**, 1816–1831.

Hoerling, M. P., Schaack, T. K. and Lenzen, A. J. 1993. A global analysis of stratospheric–tropospheric exchange during Northern winter. *Mon. Wea. Rev.* **121**, 162–172.

Holton, J. R., Haynes, P. H., McIntyre, M. E., Douglass, A. R., Rood R. B. and Pfister, L. 1995. Stratosphere–troposphere exchange. *Rev. Geophys.* **33**, 403–439.

Hoor, P., Fischer, H., Lange, L., Lelievelt, J. and Brunner, D. 2002. Seasonal variations of a mixing layer in the lowermost stratosphere as identified by the CO–O_3 correlation from *in situ* measurements. *J. Geophys. Res.* **107**, doi 10.1029/2000JD000289.

Hoskins, B., McIntyre, M. and Robertson, W. 1985. On the use and significance of isentropic potential vorticity map. *Q. J. R. Meteorol. Soc.* **111**, 877–946.

Jaffe, D., Mahura, A., Kelley, J., Atkins, J., Novelli, P. C. and Merrill, J. 1997. Impact of Asian emissions on the remote North Pacific atmosphere: Interpretation of CO data from Shemya, Guam, Midway and Mauna Loa, *J. Geophys. Res.* **102**, 28 627–28 635.

Japan Meteorological Agency (JMA) 2000. Monthly report of Meteorological Satellite Center February 2000. Meteorological Satellite Center Japan Meteorological Agency, Tokyo.

Kato, N. and Akimoto, H. 1992. Anthropogenic emissions of SO_2 and NO_x in Asia: emission inventories, *Atmos. Environ.* **26**, 2997–3017.

Kawakami, S., Kondo, Y. Koike, M., Nakajima, H., Gregory, G. L., Sachse, G. W., Newell, R. E., Browell, E. V., Blake, D. R., Rodriguez, J. M. and Merrill, J. T. 1997. Impact of lightning and convection on

reactive nitrogen in the tropical free troposphere. *J. Geophys. Res.* **102**, 28 367–28 384.

Keeling, C. D., Whorf, T. P., Wahlen, M. and van der Plicht, J. 1995. International extremes in the rate of rise of atmospheric carbon dioxide since 1980. *Nature* **375**, 666–670.

Kley, D., Crutzen, P. J., Smit, H. G. J., Vömel, H., Oltmans, S. J., Grassl, H. and Ramanathan, V. 1996. Observations of near-zero ozone concentrations over the convective Pacific: effects on air chemistry, *Science* **274**, 230–233.

Koike, M., Kondo, Y., Kawakami, S., Nakajima, H., Gregory, G. L., Sachse, G. W., Singh, H. B., Browell, E. V., Merrill, J. T. and Newell, R. E. 1997. Reactive nitrogen and its correlation with O_3 and CO over the Pacific in winter and early spring. *J. Geophys. Res.* **102**, 28 385–28 404.

Kondo, Y., Koike, M, Kawakami, S., Singh, H. B., Nakajima, H., Gregory, G. L., Blake, D. R., Sachse, G. W., Merrill, J. T. and Newell, R. E. 1997. Profiles and partitioning of reactive nitrogen over the Pacific Ocean in winter and early spring. *J. Geophys. Res.* **102**, 28 405–28 424.

Lelieveld, J., Bregman, B., Arnold, F., Bürger, V., Crutzen, P. J., Fischer, H., Waibel, A., Siegmund, P. and van Velthoven, P. F. J. 1997. Chemical perturbation of the lowermost stratosphere through exchange with the troposphere. *Geophys. Res. Lett.* **24**, 603–606.

Liu, C. M., Buhr, M. and Merril, J. T. 1997. Ground-based observations of ozone, carbon monoxide, and sulfur dioxide at Kenting, Taiwan, during PEM-West B campaign. *J. Geophys. Res.* **102**, 28 613–28 625.

Matsueda, H. and Inoue, H. Y. 1996. Measurements of atmospheric CO_2 and CH_4 using a commercial airliner from 1993 to 1994. *Atmosph. Envir.* **30**, 1647–1655.

Matsueda, H., Inoue, H. Y., Sawa, Y. and Tsutsumi, Y. 1998. Carbon monoxide in the upper troposphere over the western Pacific between 1993 and 1996. *J. Geophys. Res.* **20**, 19 093–19 110.

Matsueda, H. and Inoue, H. Y. 1999. Aircradt measurements of trace gases between Japan and Singapore in October of 1993, 1996, and 1997. *Geophys. Res. Lett.* **26**, 2413–2416.

Matsueda, H., Inoue, H. Y. and Ishii, M. 2001. Aircraft observation of carbon dioxide at 8–13 km altitude over the western Pacific from 1993 to 2001. *6th Int. Carbon Dioxide Conf., Extended Abstracts* **I**, 12–14.

Matsueda, H., Inoue, H. Y. and Ishii, M. 2002. Aircraft observation of carbon dioxide at 8–13 km altitude over the western Pacific from 1993 to 1999. *Tellus* **54B**, 1–21.

Merrill, J. T., Uematsu, M. and Bleck, R. 1989. Meteorological analysis of long-range transport of mineral aerosols over the North Pacific. *J. Geophys. Res.* **94**, 8584–8598.

Nakazawa, T., Miyashita, K., Aoki, S. and Tanaka, M. 1991. Temporal and spatial variations of upper tropospheric and lower stratospheric carbon dioxide. *Tellus* **43B**, 106–117.

Nakazawa, T., Morimoto, S., Aoki, S. and Tanaka, M. 1993. Time and space variations of the carbon isotopic ratio of tropospheric carbon dioxide over Japan. *Tellus* **45B**, 258–274.

Nakazawa, T., Morimoto, S., Aoki, S. and Tanaka, M. 1997. Temporal and spatial variations of the carbon isotopic ratio of atmospheric carbon dioxide in the western Pacific region. *J. Geophys. Res.* **102**, 1271–1285.

Novelli, P. C., Steele, L. P. and Tans, P. P. 1997. Mixing ratios of carbon monoxide in the troposphere. *J. Geophys. Res.* **97**, 20 731–20 750.

Novelli, P. C., Lang, P. M., Masarie, K. A., Hurst, D. F., Myers, R. and Elkins, J. W. 1999. Molecular hydrogen in the troposphere: Global distribution and budget. *J. Geophys. Res.* **104**, 30 427–30 444

Parrish, D. D., Trainer, M., Holloway, J. S., Yee, J. E., Warshawsky, M. S., Fehsendeld, F. C., Forbes, G. L. and Moody J. L. 1998. Relationships between ozone and carbon monoxide at surface sites in the North Atlantic region. *J. Geophys. Res.* **103**, 13 357–13 376.

Piotrowicz, S. R., Boran, D. A. and Fischer, C. J. 1986. Ozone in the boundary layer of the equatorial Pacific Ocean. *J. Geophys. Res.* **91**, 13 113–13 119.

Routhier, F., Dennett, R., Davis, D. D., Wartburg, A., Haagenson, P. and Delany, A. C. 1980. Free tropospheric and boundary layer airborne measurements of ozone over the latitude range of 58°S and 70°N. *J. Geophys. Res.* **85**, 7307–7321.

Sawa, Y., Matsueda, H., Tsutsumi, Y., Jensen, J. B., Inoue, H. Y. and Makino, Y. 1999. Tropospheric carbon monoxide and hydrogen measurements over Kalimantan in Indonesia and northern Australia during October, 1997. *J. Geophys. Lett.* **26**, 1389–1392.

Simmonds, P. G., Derwent, R. G., O'Doherty, S., Ryall, D.B., Steele, L. P., Langenfelds, R. L., Salameh, P., Wang, H. J., Dimmer, C. H. and Hudson, L. E. 2000. Continuous high-frequency observations of hydrogen at the Mace Head baseline atmospheric monitoring station over the 1994–1998 period. *J. Geophys. Res.* **105**, 12 105–12 121.

Singh, H. B., Gregory, G. L., Anderson, B., Browell, E., Sachse, G. W., Davis, D. D., Crawford, J., Bradshaw, J. D., Talbot, R., Blake, D. R., Thornton, D., Newell, R. and Merrill, J. 1996. Low ozone in the marine boundary layer of the tropical Pacific Ocean: Photochemical loss, chlorine atoms, and entrainment. *J. Geophys. Res.* **101**, 1907–1917.

Talbot, R. W., Dibb, J. E., Lefer, B. L., Bradshaw, J. D., Sandholm, S. T., Blake, D. R., Blake, N. J., Sachse, G. W., Collins, J. E., Jr, Heikes, B. G., Merrill, J. T., Gregory, G. L., Anderson, B. E., Singh, H. B., Thornton, D. C., Brandy, A. R. and Pueschel, R. F. 1997. Chemical characteristics of continental outflow from Asia to the troposphere over the western Pacific Ocean during February–March 1994: result from PEM-West B. *J. Geophys Res.* **102**, 28 255–28 274.

Tanaka, M., Nakazawa, T. and Aoki, S. 1987. Time and space variations of tropospheric carbon dioxide over Japan. *Tellus* **39B**, 3–12.

Yonemura, S., Yokozawa, M., Kawashima, S. and Tsuruta, H. 2000. Model analysis of the influence of gas diffusivity in soil on CO and H_2 uptake. *Tellus* **52B**, 919–933.

Wild, O. and Akimoto, H. 2001. Intercontinental transport of ozone and its precursors in a three-dimensional global CTM. *J. Geophys. Res.* **106**, 27 729–27 774.

Wofsy, S. C., Boering, K. A., Daube, B. C. Jr, and McElroy, M. B. 1994. Vertical transport rates in the stratosphere in 1993 from observations of CO_2, N_2O, and CH_4. *Geophys. Res. Lett.* **21**, 2571–2574.

Wu, Z., Newell, R. E., Zhu, Y., Anderson, B. E., Browell, E. V., Gregory, G. L., Sachse, G. W. and Collins, J. E., Jr, 1997. Atmospheric layers measured from the NASA DC-8 during PEM-West B and comparison with PEM-West A. *J. Geophys. Res.* **102**, 28 353–28 365.

Zahn, A., Neubert, R., Maiss, M. and Platt, U. 1999. Fate of long-lived trace species near the Northern Hemispheric tropopause: Carbon dioxide, methane, ozone, and sulfur hexafluoride. *J. Geophys. Res.* **104**, 13 923–13 942.

Zahn, A., Brenninkmeijer, C. A. M., Maiss, M. Maiss, Schartffe, D. H., Crutzen, P. J., Hermann, M., Heintzenberg, J., Wiedensohler,

A., Güsten, H., Heinrich, G., Fischer, H., Cuijpers, J. W. M. and van Velthoven, P. F. J. 2000. Identification of extropical two-way troposphere–stratosphere mixing based on CARIBIC measurements of O_3, CO, and ultrafine particles. *J. Geophys. Res.* **105**, 1527–2535.

Zahn, A., Brenninkmeijer, C. A. M., Asman, W. A. H., Crutzen, P. J., Heinrich, G., Fischer, H., Cuijpers, J. W. M. and van Velthoven, P. F. J. 2002. Budgets of O_3 and CO in the upper troposphere: CARIBIC passenger aircraft results 1997–2001. *J. Geophys. Res.* **107**, doi 10.1029/2001JD001529.